

# DEVELOPMENT OF Nb<sub>3</sub>Sn COATINGS ON COPPER AT INFN-LNL\*

D. Fonnesu<sup>†1</sup>, E. Chyhyrynets<sup>1</sup>, D. Ford<sup>1</sup>, S. Keckert<sup>2</sup>, J. Knobloch<sup>2,6</sup>, F. Kramer<sup>2</sup>, O. Kugeler<sup>2</sup>, M. Lazzari<sup>1</sup>, G. Marconato<sup>3</sup>, I. Curci<sup>4</sup>, T. Proslie<sup>5</sup>, M. Wenskat<sup>3,7</sup>, A. Zubtsovskii<sup>6</sup>, C. Pira<sup>1</sup>

<sup>1</sup>INFN National Institute for Nuclear Physics - Legnaro National Laboratories, Legnaro, Italy

<sup>2</sup>HZB Helmholtz-Zentrum Berlin for Materials and Energy, Berlin, Germany

<sup>3</sup>University of Hamburg, Hamburg, Germany

<sup>4</sup>Université Paris-Saclay, Gif-sur-Yvette, France

<sup>5</sup>CEA French Alternative Energies and Atomic Energy Commission, Paris-Saclay, France

<sup>6</sup>University of Siegen, Siegen, Germany

<sup>7</sup>DESY German Electron Synchrotron, Hamburg, Germany

## Abstract

The successful development of Nb<sub>3</sub>Sn/Cu coatings for the SRF cavities of next generation particle accelerators would result in the reduction of the needed cryogenic power by a factor 3 with respect to what normally needed for bulk Nb cavities, while maintaining operation at 4.5 K. In the framework of the IFAST and ISAS collaborations, research activities are carried out at INFN-LNL to develop new technologies for the application of Nb<sub>3</sub>Sn on Cu, including seamless spinning of cavity prototypes, surface chemical preparation, cavity coating and testing. At the same time, an optimized recipe for Nb<sub>3</sub>Sn films deposited via DCMS has been established on flat samples and is discussed in this work. The recipe delivers films showing a  $T_c \approx 17$  K, at deposition temperatures  $\leq 650$  °C, on a Cu substrate pre-coated with a 30  $\mu\text{m}$ -thick buffer layer of Nb. The deposition recipe has been validated on bulk Nb by measuring its RF properties on a QPR sample, with the results being also discussed in this work. A surface resistance of 23 n $\Omega$  at 4.5 K and 20 mT is measured, which corresponds to a  $Q_0$  about 5 times larger than the baseline specification for the LHC Nb/Cu cavities and already fulfills the requirements for the FCC-ee. Finally, updates on the activities toward the scalability of the coating recipe to the 1.3 GHz elliptical cavity prototype are given, and the perspectives for further coating recipe refinement are discussed.

## INTRODUCTION

The development of next-generation particle accelerators, such as the FCC-ee, imposes stringent requirements on energy efficiency [1]. For superconducting RF (SRF) accelerating cavities, the class-A15 intermetallic compound Nb<sub>3</sub>Sn is a promising superconducting (SC) material alternative to Nb. Its high critical temperature (18.3 K against 9.2 K of Nb) corresponds to a BCS surface resistance  $R_{BCS}$  at 4.5 K comparable to that of Nb at 2 K [2], and lower than that of Nb films on Cu at 4.5 K [3], enabling operation at 4.5 K with

significantly reduced cryogenic costs. However, the brittleness of Nb<sub>3</sub>Sn makes bulk machining impractical, limiting its application to thin-film coatings.

The state-of-the-art technique for Nb<sub>3</sub>Sn cavities is vapour tin diffusion (VTD), whose best performance showed a quality factor  $Q_0 \approx 10^{10}$  at 4.4 K up to 20 MV m<sup>-1</sup> for 650 MHz cavities [4]. Despite these results, VTD relies on a bulk Nb substrate, much pricier than Cu (RRR = 300 niobium  $\approx$  100x more expensive than OFHC Cu) [5], making it less appealing, in terms of costs, for large-scale cavity production. The technique is also prone to the formation of sub-stoichiometric phases [6], undesired as they contribute to the degradation of the RF performance. Last, but not least important, the copper substrate introduces several advantages with respect to bulk Nb, in addition to its cost: it has higher thermal conductivity than bulk Nb at 4.5 K, and potentially allows cryocooler-based conduction cooling (9 W cooling power recently demonstrated at 4.2 K [7, 8]). This makes physical vapour deposition (PVD) a technique of high interest for the production of Nb<sub>3</sub>Sn films on Cu for SRF cavities. In fact, a successful development of Nb<sub>3</sub>Sn coatings on copper would make possible to cover the current baseline requirements for the SRF cavities of FCC-ee [9], for both the main ring and the booster, for which Nb/Cu and bulk Nb cavities are, respectively, currently foreseen.

In this context, a baseline deposition recipe for Nb<sub>3</sub>Sn films on copper has been established via direct current magnetron sputtering (DCMS) at INFN-LNL, via a  $T_c$ -driven study [10]. The experimental methods to pursue this result, to advance the analysis of the morphological, thermal, and superconducting properties of these coatings, and to scale-up the deposition recipe to a 1.3 GHz cavity prototype are described in the Experimental Methods Section. The DCMS deposition recipe will be discussed in Results and Discussion, along with the most recent results in terms of the above-mentioned characterizations, and progress toward the making of the first Nb<sub>3</sub>Sn/Cu 1.3 GHz cavity.

## EXPERIMENTAL METHODS

### $T_c$ -driven DCMS Deposition Recipe Optimization

The production and characterization of the Nb<sub>3</sub>Sn film samples produced for the optimization of the DCMS depo-

\* This research was partly supported by the European Union's Horizon-INFRA-2023-TECH-01 under GA No 101131435 - iSAS, the European Union's Horizon 2020 Research and Innovation programme under GA No 101004730 - IFAST, the INFN CSN5 experiment SuperMAD, the INFN CSN1 experiment RD FCC, and the INFN ESPP project SRF.

<sup>†</sup> fonnesu@infn.it

sition recipe was carried out according to a standardized procedure. The parameters for the optimized recipe are given in Results and Discussion. After each deposition, the samples undergo the following characterization procedure:

- measurement of  $T_c$  via contactless, inductive method;
- assessment of the surface morphology via SEM;
- measurement of the Nb-Sn composition via EDS;
- assessment of the crystalline structure via XRD.

These were all part of the tight-feedback standardized loop process established for the development of the DCMS recipe.

All the custom samples produced for the measurements discussed in this paper have been deposited according to the optimized recipe and also characterized according to this same standard procedure.

### RF Measurements

The RF characterization of the films has been performed using the quadrupole resonator (QPR) facility [11, 12] at HZB (Berlin, Germany). The QPR is a dedicated sample test cavity designed to measure the RF surface resistance  $R_S$  of SC samples. It consists of a cylindrical cavity made of high-RRR Nb, with two pole-shoe-shaped Nb pipes positioned at less than 1 mm distance from the surface of an interchangeable sample. The latter consists of a cylindrical substrate of 100 mm diameter and 100 mm height, prepared from high-RRR Nb and coated with a  $\geq 1 \mu\text{m}$  Nb<sub>3</sub>Sn film on the flat top surface and on the lateral surface for the measurement presented in this work.

The cavity is immersed in superfluid He-4, which also cools the pole shoes from the inside. The resonator excites quadrupole-like modes at 417 MHz, 850 MHz, and 1300 MHz, localized at the gap between the pole shoes and the sample surface, which induce RF currents in the sample. The sample is thermally decoupled from the resonator via a coaxial line, allowing direct measurements of RF dissipation (and hence  $R_S$ ) using a calorimetric RF-DC compensation technique with a heater and a temperature sensor placed at the bottom of the sample. Surface resistance measurements can be conducted at high RF fields up to 120 mT and arbitrary sample temperatures above the minimum liquid He bath temperature of 1.5 K. Additionally, the QPR enables measurements of other relevant parameters, including  $T_c$ , RF quench field and London penetration depth  $\lambda_L$ . A detailed description of the experimental setup and measurement techniques is found in [13].

### Flux Trapping Measurements

Possible magnetic flux trapping phenomena have been also assessed at HZB. The facility for flux trapping measurement consists of a liquid He bath cryostat, inside which the experimental setup lies on top of the bath in He vapor. The sample prepared for this measurement is a  $100 \times 60 \times 3 \text{ mm}^3$  OFHC Cu slab, coated with a  $30 \mu\text{m}$  thick Nb buffer layer and

a  $1 \mu\text{m}$  thick Nb<sub>3</sub>Sn film on top. The two far ends of the sample are clamped at two Cu blocks, each connected to heaters for precise control of the cool-down rate and of the temperature gradient across the sample. Three coils around the cryostat compensate Earth's magnetic field and expose the sample to a static, controlled magnetic field. The temperature gradient and distribution across the sample is monitored via sensors distributed along the sample length, and multiple AMR sensors distributed on the sample back surface are employed for magnetic field measurements. More details about the measurement setup can be found in [14].

### SC Energy Gap Measurements

Measurements of the SC energy gap have been performed by a point contact tunneling spectroscopy (PCTS) device at CEA (Paris-Saclay, France). By probing the SC density of states (DOS), PCTS allows to study the surface SC properties of samples or real devices, such as SRF cavities, and has the capability of studying the native oxide layer/tunnel barrier itself, which is often present, and may contain defects relevant to the performance limitation of SC devices. The PCTS apparatus at CEA enables a controlled and automatic motion of the probe-tip with respect to the fixed sample, granting high-precision control of the junction resistance, that can be measured from a quasi-ohmic regime (few hundred Ohms) to a tunnel regime (up to 1 G $\Omega$ ). It also allows mapping of the sample surface SC properties on lateral (X,Y) scales ranging from tens of  $\mu\text{m}$  up to mm. The details about the measurement setup can be found in [15]. The sample prepared for this measurement consisted of a small  $20 \times 10 \times 0.5 \text{ mm}^3$  OFHC Cu *coupon* coated with a  $30 \mu\text{m}$  Nb buffer layer and a Nb<sub>3</sub>Sn  $1 \mu\text{m}$  thick film on top.

### Thermal Transmittance Measurements

The thermal transmittance measurements of the Nb<sub>3</sub>Sn films deposited on Cu has been measured at DESY (Hamburg, Germany). The experimental setup is made to induce a controlled heat flux through the sample and measure the resulting temperature gradient across it in an equilibrium condition. It consists of a superfluid He-4 leak-tight cylindrical cell with two identical study sample disks mounted on either sides. A wire heater and a thermometer are installed inside the cell, placed in a superfluid He-4 bath. The measurement station and method are described in detail in [16]. The samples prepared for this measurement consisted of two OFHC Cu disks of 45 mm diameter and 2.6 mm thickness, coated with a  $30 \mu\text{m}$  thick Nb buffer layer and a  $1 \mu\text{m}$  thick Nb<sub>3</sub>Sn film on top.

### Scalability

The scalability of the optimized DCMS deposition recipe is being pursued by the construction of a custom deposition system for the coating of a 1.3 GHz prototype elliptical cavity. A complete UHV-compatible sputtering system has been successfully designed, assembled, and tested at INFN-LNL, and is conceived to reproduce the critical conditions

required for high-quality  $\text{Nb}_3\text{Sn}$  growth via DCMS, especially low power density and high substrate temperature, demonstrated on small samples. The design consists of an innovative fixed-magnetron with rotating cavity system. The main addressed challenges included the implementation of a compact, all-metal planar magnetron compatible with the cavity geometry, the integration of a high-efficiency heating system based on infrared lamps, and the development of a custom sealing technique ensuring mechanical robustness and vacuum integrity without resorting to brazing.

## RESULTS AND DISCUSSION

At INFN-LNL, a baseline deposition recipe for  $\text{Nb}_3\text{Sn}$  films on copper has been established via direct current magnetron sputtering (DCMS). It can be condensed in the following set of parameters and conditions:

- sputtering gas (Ar) pressure:  $2 \times 10^{-2}$  mbar
- target surface current density:  $\leq 1 \text{ mA cm}^{-2}$
- substrate temperature:  $\leq 650 \text{ }^\circ\text{C}$
- no post-deposition annealing
- Nb buffer layer thickness:  $\geq 30 \text{ } \mu\text{m}$  (NbBL-30)

The surface current density at the target and the thickness of the NbBL have been key parameters for the successful achievement of a DCMS optimized deposition recipe. This way,  $\text{Nb}_3\text{Sn}$  films on Cu pre-coated with a NbBL-30 exhibiting  $T_c \approx 17 \text{ K}$  have been obtained.

This optimized coating has been RF tested on bulk Nb substrate at the HZB QPR facility. The  $T_c$  of 17.2 K measured for the film, via frequency shift and quench field measurement, is consistent with the one obtained on small samples and measured at LNL via inductive method. As shown in Fig. 1, the film exhibited a surface resistance  $R_s$  of 23 n $\Omega$  at 4.5 K and at 20 mT (at 417 MHz).

The data obtained during the fast cooldown are better or comparable to the  $R_s$  measured for a sample produced via VTD up to 40 mT, above which a steep rise is observed, likely linked to thermal dissipation. The  $R_s$  measured during a slow cooldown resulted systematically larger than the one obtained during the slow cooldown, in turn hinting to trapped magnetic flux in the film. A quench field of  $\sim 70 \text{ mT}$  has been measured for this film (100 mT for the VTD sample [11]), also possibly due to flux trapping.

A sample of  $\text{Nb}_3\text{Sn}$  on a NbBL-30/Cu substrate has been prepared for flux trapping measurement, also at HZB. Figure 2 shows the dependence of the trapped magnetic flux against the temperature gradient along the sample's length. Before the measurement, the Earth's magnetic field ( $< 2 \text{ } \mu\text{T}$ ) has been compensated via Helmholtz coils. At the minimum temperature gradient, the measured trapped flux is of 30  $\mu\text{T}$ , and rises up to 500  $\mu\text{T}$  for a gradient of 200 mK/cm. This is, with all likelihood, an effect of thermo-electric currents induced in the copper substrate during cooldown. A sample

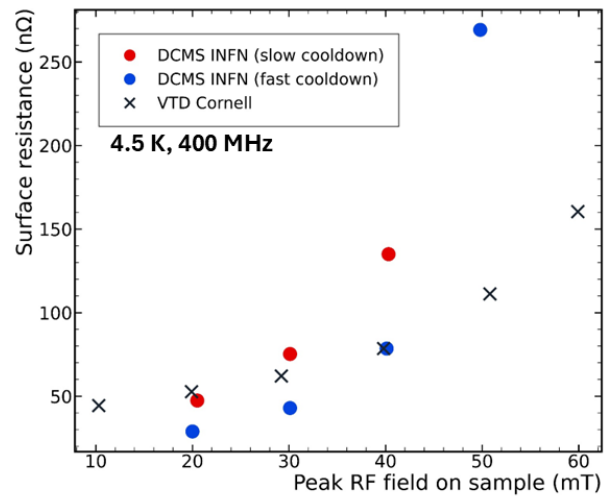


Figure 1: Surface resistance of the LNL optimized coating on bulk Nb compared to a Cornell sample produced by VTD (state of the art).

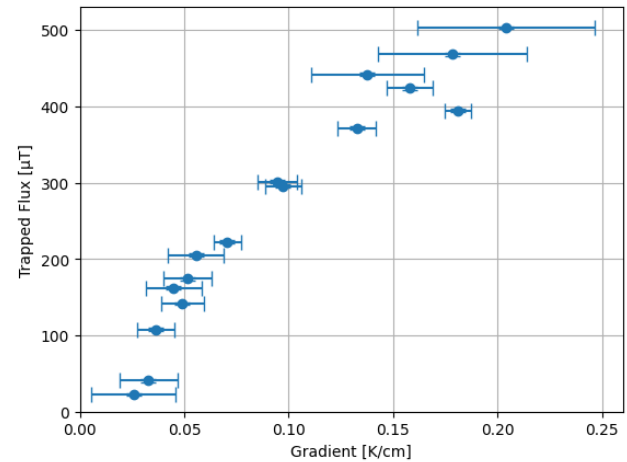


Figure 2: Trapped flux measured versus the temperature gradient along the sample for a  $\text{Nb}_3\text{Sn}$  coating deposited at LNL on copper pre-coated with a 30  $\mu\text{m}$  thick Nb buffer layer.

on bulk Nb is planned to be measured next for a direct comparison with what observed on the cooldown dependence of the QPR data.

The SEM micrographs of the coatings point out a dependence of their surface morphology on the substrate type. Figure 3 shows a  $\text{Nb}_3\text{Sn}$  film deposited according to the optimized recipe on bulk Nb (left) and on a NbBL-30/Cu substrate (right). The film on bulk Nb exhibits *island*-like formations which disrupt the homogeneity of the surface. On the other hand, the film on NbBL shows regular, large grains of consistent appearance. When assessed via EDS, the average film composition falls in the range 23 – 25 At% of Sn. However, a punctual analysis of the *islands* and of the base film reveals that, although the stoichiometry of the

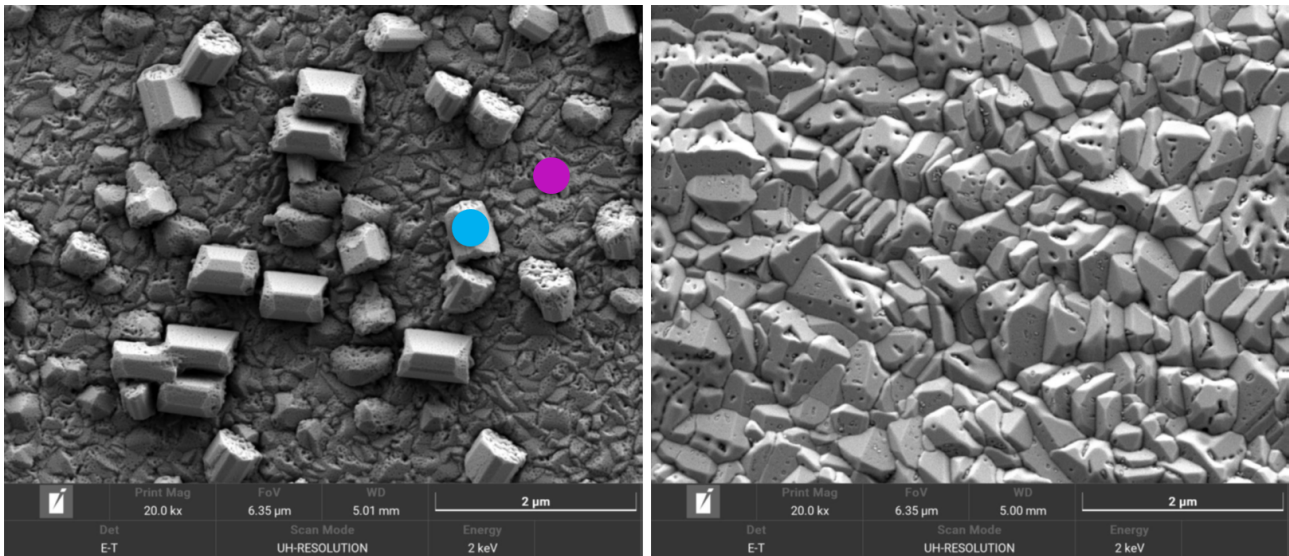


Figure 3: SEM micrographs of a  $\text{Nb}_3\text{Sn}$  coating on bulk Nb substrate (left) and on NbBL-30/Cu substrate (right). The blue and purple dots indicate example areas where the ESD punctual analysis has been performed, whose results are given in Fig. 4.

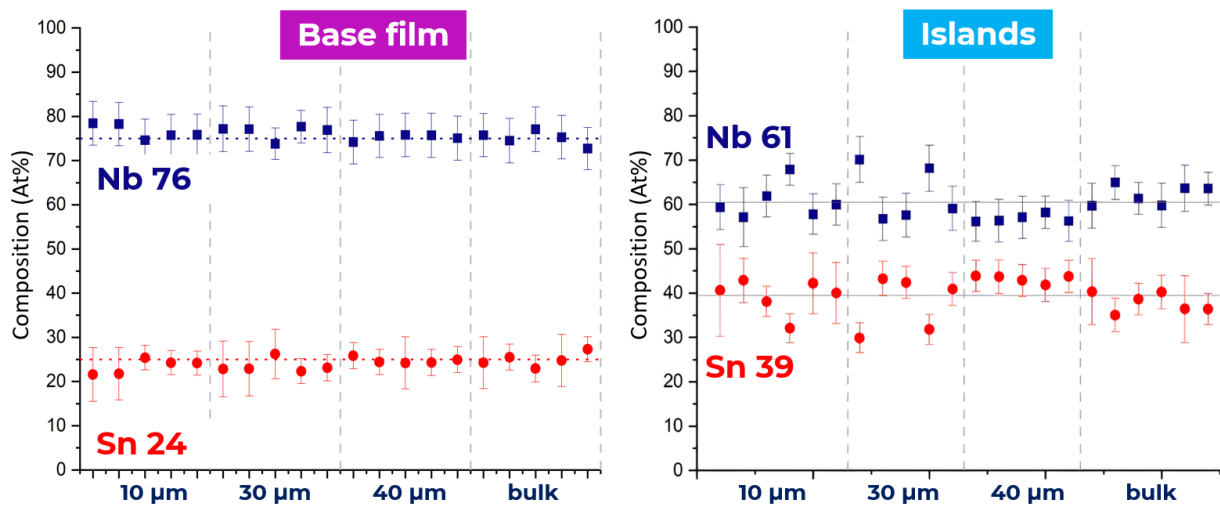


Figure 4: EDS punctual analysis of base film (left) and island (right) areas performed for coatings on different substrates.

latter stays overall balanced, the *islands* exhibit an excess of Sn, as shown in Fig. 4.

Their non-stoichiometric composition and their structure itself are likely to be the main cause for the observed resistive losses in RF environment.

The SC energy gap of the coating on NbBL-30/Cu has been measured at CEA, and resulted into  $\Delta = (2.47 \pm 0.27)$  meV. This is lower than the value expected from literature [17, 18] due to the lower sample  $T_c$  of about 16 K. As shown in Fig. 5 (central column), despite a lower value the distribution of gap values is well peaked and shows an almost complete absence of sub-gaps. The measurement of a sample on bulk Nb substrate has been also attempted, but turned out to be undoable because of the presence of the Sn-rich island structures.

For comparison, samples produced at CERN via HiPIMS (Fig. 5 (left column)) and FNAL via VTD (Fig. 5 (right column)) exhibit a peak value which is comparable to the sample produced at LNL in the case HiPIMS sample, and better (about 3 meV) for the VTD sample. However, both these samples exhibit a wide distribution of sub-gap values.

To assess the impact of a thick Nb buffer layer on the thermal transmittance of the substrate, the latter has been measured at the dedicated experimental setup at DESY. Figure 6 shows the thermal transmittance measured for a pair of  $\text{Nb}_3\text{Sn}/\text{NbBL-30}/\text{Cu}$  and  $\text{Nb}_3\text{Sn}/\text{Cu}$  disks at 2 K and 1.8 K, and 1.8 K only respectively. Both disk pairs demonstrated, at both temperatures, better transmittance than the bulk Nb baseline at 2 K. The thermal effect of the NbBL is anyway visible when comparing the samples with and without

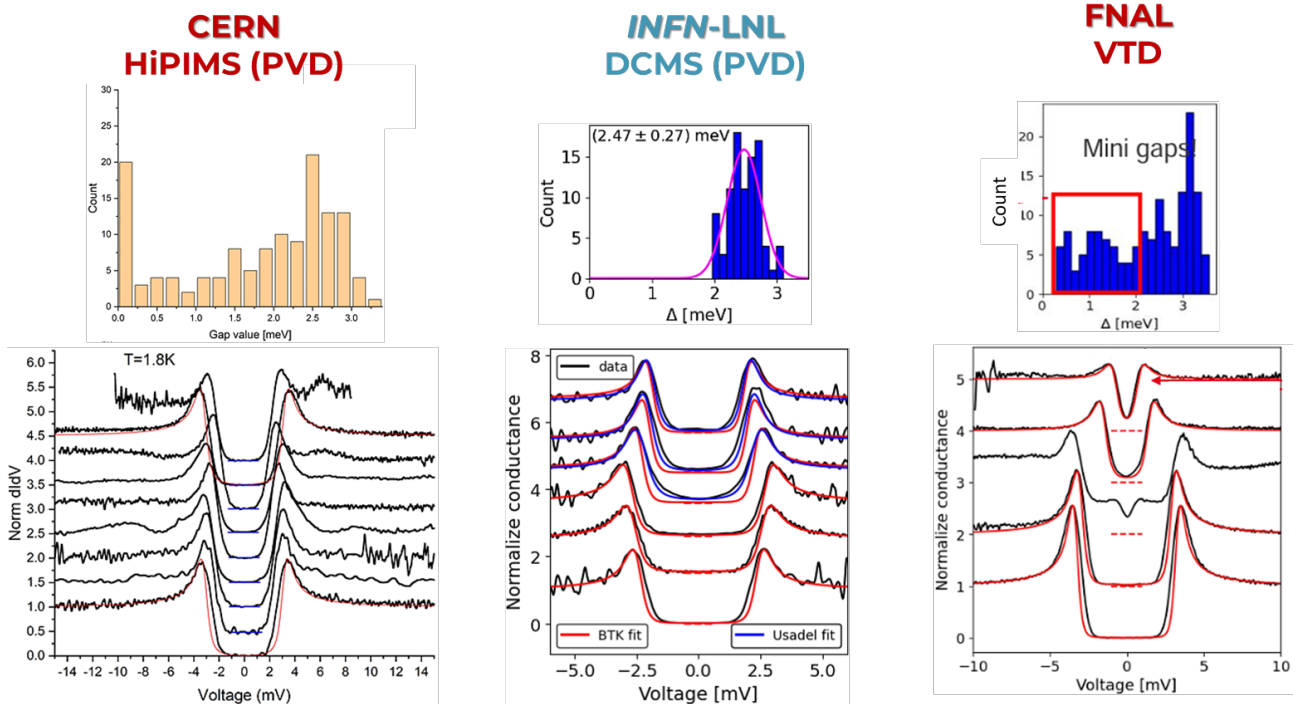


Figure 5: Superconducting gap measurements compared. From left to right: CERN sample produced via HiPIMS on Cu with Ta buffer layer, LNL sample produced via DCMS on Cu with Nb buffer layer, FNAL sample produced via VTD.

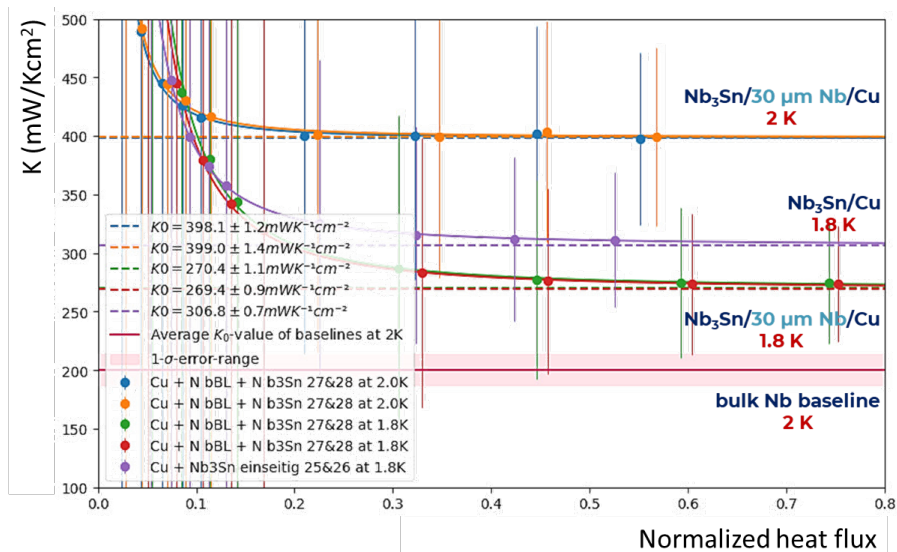


Figure 6: Thermal transmittance measurements of Nb<sub>3</sub>Sn samples deposited at LNL on Cu and on NbBL-30, compared to the bulk Nb baseline.

NbBL-30 measured at 1.8 K, for which the transmittance is partly worsened by the presence of the buffer layer.

Finally, the process to scale-up the DCMS optimized coating to 1.3 GHz prototypes is being carried on in parallel at STFC and LNL within the framework of the IFAST program. The two institutes are pursuing complementary designs. At STFC a fixed-cavity system with two 2" planar magnetron movable along the cavity axis has been made and successfully tested, and the first bulk Nb cavity has been recently

coated. The inner cavity before and after the coating, and a schematics of system depicting only one of the two magnetrons is given in Fig. 7. At LNL, a rotating-cavity system with fixed rectangular magnetron has been assembled and tested, with a first successful ignition of the Nb plasma being the most recent result. Figure 8 shows the system design and a real-life picture of the first ignited plasma.

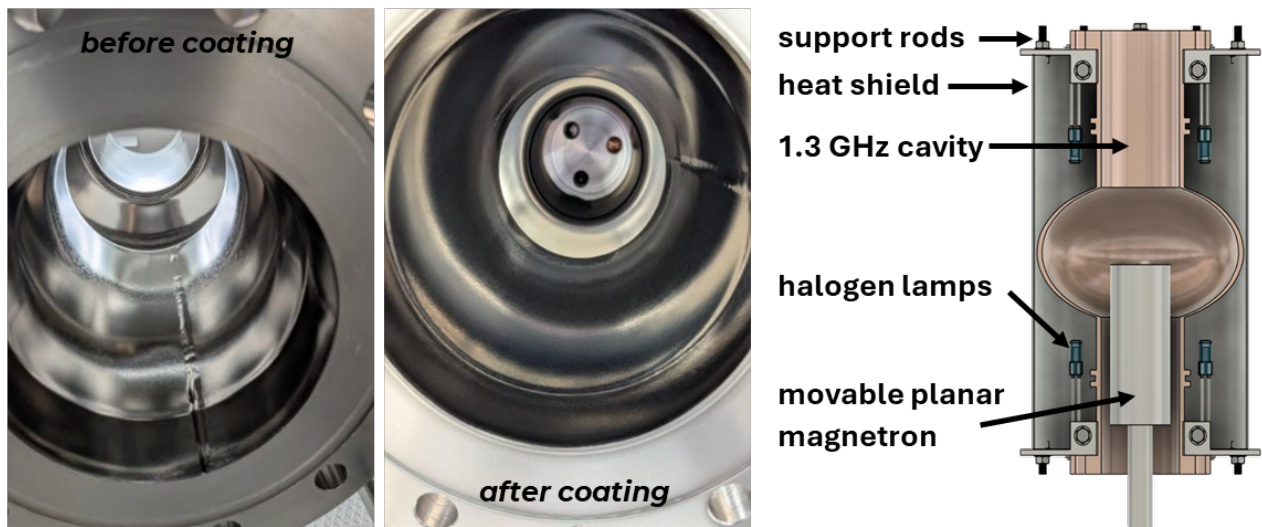


Figure 7: 1.3 GHz bulk Nb cavity before and after  $\text{Nb}_3\text{Sn}$  deposition with the STFC sputtering system (on the right).

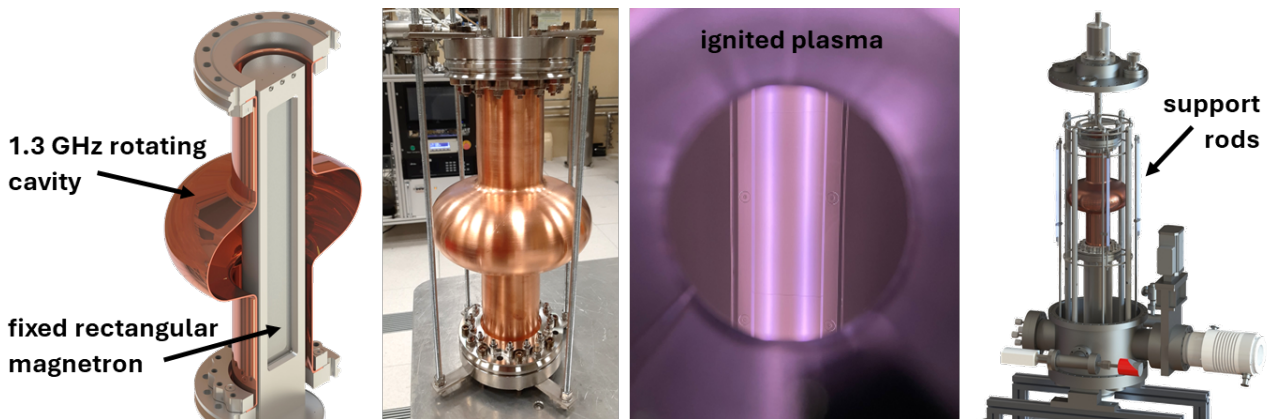


Figure 8: Sputtering system for 1.3 GHz cavities under development at INFN-LNL.

## CONCLUSION

A baseline coating recipe for  $\text{Nb}_3\text{Sn}$  thin films on copper has been successfully established at INFN-LNL using DC magnetron sputtering. The optimized parameters, such as low target current density, deposition temperature  $\leq 650^\circ\text{C}$ , and a Nb buffer layer (NbBL) of thickness  $\geq 30\ \mu\text{m}$ , enable the reproducible growth of films with  $T_c \approx 17\ \text{K}$  and near-stoichiometric composition.

The RF test on bulk Nb substrate confirmed the effectiveness of the recipe, yielding a surface resistance of  $23\ \text{n}\Omega$  at 4.5 K, 400 MHz, and 20 mT, corresponding to a  $Q_0$  about five times higher than the Nb/Cu baseline for LHC cavities and already meeting FCC-ee requirements. At the same time, morphological studies revealed that Sn-rich islands, observed on bulk Nb but mostly suppressed on Nb buffer layer, are likely responsible for additional RF losses. The Nb buffer layer also impacts thermal transport, slightly reducing transmittance compared to bare Cu, but overall still outperforming bulk Nb at cryogenic temperatures.

Complementary characterizations, including tunneling spectroscopy and flux trapping measurements, further high-

light the importance to avoid stoichiometry and morphology imbalances, and to understand their relation to the coating RF properties. To allow direct comparison with the QPR results, samples on bulk Nb are planned to be prepared soon for flux trapping measurements.

Finally, work is now progressing toward the coating of full 1.3 GHz elliptical cavities using newly developed sputtering systems at INFN-LNL and STFC, with the latter having recently performed the first coating on a bulk Nb cavity.

These results demonstrate that  $\text{Nb}_3\text{Sn}/\text{Cu}$  coatings via DCMS are a promising and possibly scalable way toward efficient SRF cavities, combining high performance at 4.5 K with the cost and thermal advantages of the copper substrate. Ongoing efforts will focus on further mitigating Sn-rich inhomogeneities, refining buffer layer design by investigating pulsed deposition techniques, and validating cavity coatings under RF conditions.

## REFERENCES

- [1] C. Adolphsen *et al.*, “European Strategy for Particle Physics - Accelerator R&D Roadmap”, CERN, Geneva, Switzerland, CERN Yellow Reports: Monographs, 2022. doi:10.23731/CYRM-2022-001
- [2] I.FAST WP9 Members, “Thin-Film SRF Roadmap Report”, CEA, Gif-sur-Yvette, France, Tech Rep. Deliverable D9.1, 2025. <https://zenodo.org/records/14731412>
- [3] C. Benvenuti *et al.*, “Study of the surface resistance of superconducting niobium films at 1.5 GHz”, *Physica C*, vol. 316, no. 3-4, 1999. doi:10.1016/S0921-4534(99)00207-5
- [4] S. Posen *et al.*, “Advances in Nb3Sn superconducting radiofrequency cavities towards first practical accelerator applications”, *Supercond. Sci. Technol.*, vol. 34, no. 2, Jan. 2021. doi:10.1088/1361-6668/abc7f7
- [5] Metal.com website, [www.metal.com](http://www.metal.com)
- [6] S. A. Willson *et al.*, “Impact of Submicron Nb3Sn Stoichiometric Surface Defects on High-Field Superconducting Radiofrequency Cavity Performance”, *Phys. Rev. Res.*, vol. 6, no. 4, Nov. 2024. doi:10.1103/PhysRevResearch.6.043133
- [7] X. Hao *et al.*, “Development of a 5 W/4.2 K Two-Stage Pulse Tube Cryocooler”, *IOP Conf. Ser.: Mater. Sci. Eng.*, vol. 1301, no. 1, 2024. doi:10.1088/1757-899X/1301/1/012140
- [8] SHI Cryogenics Group Releases World’s Highest-Capacity 4K Cryocooler, <https://shicryogenics.com/shi-cryogenics-group-releases-worlds-highest-capacity-4k-cryocooler/>.
- [9] The FCC Collaboration, “FCC-ee: The Lepton Collider: Future Circular Collider Conceptual Design Report Volume 2”, *The European Physical Journal Special Topics*, vol. 228, no. 2, Jun. 2019. doi:10.1140/epjst/e2019-900045-4
- [10] D. Fomesu *et al.*, “Recipe Optimization and SRF Test of Cu-compatible Nb3Sn Films by DC Magnetron Sputtering from a Stoichiometric Target”, *Nature Scientific Reports*, to be published. doi:10.21203/rs.3.rs-7516819/v1
- [11] S. Keckert *et al.*, “Critical Fields of Nb3Sn Prepared for Superconducting Cavities”, *Supercond. Sci. Technol.*, vol. 32, no. 7, 2019. doi:10.1088/1361-6668/ab119e
- [12] S. Keckert *et al.*, “Mitigation of Parasitic Losses in the Quadrupole Resonator Enabling Direct Measurements of Low Residual Resistances of SRF Samples”, *AIP Advances*, vol. 11, no. 12, Dec. 2021. doi:10.1063/5.0076715
- [13] S. Keckert *et al.*, “Characterizing Materials for Superconducting Radiofrequency Applications-A Comprehensive Overview of the Quadrupole Resonator Design and Measurement Capabilities”, *Rev. Sci. Instrum.*, vol. 92, no. 6, Jun. 2021. doi:10.1063/5.0046971
- [14] F. Kramer *et al.*, “A new experiment to enable rapid systematic investigations of flux trapping dynamics for superconducting radio-frequency cavity applications”, *Rev. Sci. Instrum.*, vol. 95, no. 9, Sep. 2024. doi:10.1063/5.0202546
- [15] N. Groll *et al.*, “Point contact tunneling spectroscopy apparatus for large scale mapping of surface superconducting properties”, *Rev. Sci. Instrum.*, vol. 86, Sep. 2015. doi:10.1063/1.4931066
- [16] M. Wenskat *et al.*, “Thermal transmittance measurements of niobium at cryogenic temperatures”, *Physica C*, vol. 632, 2025. doi:10.1016/j.physc.2025.1354694
- [17] D.R. Bosomworth and G.W. Cullen, “Energy Gap of Superconducting Nb3Sn”, *Phys. Rev.*, vol. 160, no. 346, 1967. doi:10.1103/PhysRev.160.346
- [18] A. Godeke, “A review of the properties of Nb3Sn and their variation with A15 composition, morphology and strain state”, *Supercond. Sci. Technol.*, vol. 19, no. 8, Jun. 2006. doi:10.1088/0953-2048/19/8/R02